EUROPEAN COMMISSION

Community research

BELBaR

(Contract Number: 295487)

DELIVERABLE (D-N°:4.10)

Different mechanisms governing the colloidal stability of dispersions of natural bentonite in dilute solutions

Author(s): Longcheng Liu, Luis Moreno and Ivars Neretnieks
Royal Institute of Technology, Stockholm, Sweden

Reporting period: e.g. 01/09/13 – 28/02/15

Date of issue of this report: **27/10/15**

Start date of project: **01/03/12** Duration: 48 Months

Project co-funded by the European Commission under the Seventh Euratom Framework Programme for Nuclear Research &Training Activities (2007-2011)		
Dissemination Level		
PU	Public	X
RE	Restricted to a group specified by the partners of the BELBaR project	
CO	Confidential, only for partners of the BELBaR project	

EURATOM

DISTRIBUTION LIST

Name	Number of copies	Comments
Christophe Davies (EC) BELBaR participants		

Table of content

Abstract

In this report, a review is made on some important mechanisms and factors that govern or influence colloidal stability of dispersions of natural bentonite in dilute solutions. The focus is put on discussions of the pH-dependence of edge charge density of montmorillonite particles, the delamination of montmorillonite particles into small stacks of sheets upon water uptake, the different modes of colloidal coagulation, the sol-gel transition and floc formation. The effects of ion-ion correlations, discrete surface charges, and stacked sheets on swelling of bentonites are also brought out. In addition, a great deal of both experimental and theoretical studies is given for the formation of montmorillonite stacks in clay dispersions, the estimation of critical coagulation concentrations, the swelling pressure of bentonite-based materials, the upward expansion of initially compacted bentonite in a vertical test tube, and the erosion of bentonite through a fracture with seeping water of low ionic strength.

Executive summary

"The main aim of the BARBaR project is to reduce the uncertainties in the description of the effect of clay colloids on the long term performance of the engineered barrier and on radio-nuclide transport". This is to be done by:

1) "Improving the understanding of when bentonite colloids are unstable".
and by:
2) "Improving the quantitative models for erosion on the bentonite barrier for the cases when the colloids are stable".

This report mainly describes how the understanding of 1) has increased by our investigations and research. The report also shows how the improved understanding has been used to 2) improve the quantitative models for bentonite erosion from clay buffers used to protect waste canisters and tunnels. The improved models and their validation against experiments are described in three other reports reported in BELBaR Work Package 5.

Based on our contributions (Liu, 2010; Liu, 2013; Liu, 2015; Liu et al., 2009a; Liu et al., 2009b; Liu et al., 2011; Moreno et al., 2011; Neretnieks, 2009; Neretnieks, 2015; Neretnieks et al., 2009; Neretnieks et al., 2015a; Neretnieks et al., 2015b; Wang et al., 2011) to the research area of colloidal stability of clay dispersions and bentonite erosion, a review is made in the report on different mechanisms and factors that govern or influence colloidal stability of dispersions of natural bentonite in dilute solutions. Of special importance is that by using density functional theory, DFT, now it is possible to explain and quantitatively predict how the presence and concentration of multivalent counter-ions cause the semctite sheets to form stacks, a phenomenon that long has been observed experimentally, This has a strong impact on erosion properties of bentonite at the clay/water interface.

Another important finding is that in highly compacted bentonites an important contribution to the swelling pressure is that caused by crystalline swelling, which previously was not quantified in the models.

In this report we specially bring out the importance of the delamination of montmorillonite particles, the card-house mode of aggregation, the sol-gel transition, and the floc formation in determining the stability of colloidal clay dispersions and how this impacts the erosive loss of compacted bentonite into fractures that intersect deposition holes for high-level nuclear waste. Experimental as well as theoretical studies on the process of the extrusion and erosion of bentonite into fractures with seeping water are also discussed in some detail in support of the improved modeling.

1 Introduction

Bentonite is envisaged in several countries as buffer and backfill materials for nuclear waste repositories due to its favorable physical and chemical properties. In Sweden, two types of bentonite have been considered as candidates, in the KBS-3 disposal concept, to be placed around the waste canisters in a highly compacted state (SKB, 2006). One is natural Na-bentonite of Wyoming type (MX-80), in which exchangeable ions are mostly sodium. The other is natural Ca-bentonite from Milos (Deponit CA-N), which is rich in calcium.

The main constituent of natural bentonite, i.e. montmorillonite, is a member of the smectite family (van Olphen, 1977). It is a 2:1 layered sheet of aluminosilicate, built up of a central octahedral layer sandwiched by two tetrahedral layers, with the characteristic property that it swells strongly when it takes up water. As a result, stable sol may be formed in fractures that intersect deposition holes with seeping groundwater of low ionic strengths, giving rise to considerable loss of bentonite under such unfavorable conditions when the flow rate of groundwater is high (Neretnieks et al., 2009). Hence, for the sake of safety and performance assessments, it is important to adequately evaluate the behavior and properties of swelling and to assess the rate of erosion of compacted bentonite as it expands into fractures and turns from a gel into a sol in low ionic strength groundwaters. Towards that end, we discuss in this report different mechanisms and factors that govern or influence colloidal stability of dispersions of natural bentonite in dilute solutions, and both experimental and theoretical studies related to the process of the extrusion and erosion of bentonite into fractures with seeping, low ionic strength water.

In Section 2, the colloidal properties of bentonite are briefly summarized. In Section 3, the phenomena and the reason for delamination of montmorillonite particles into small stacks of sheets in colloidal clay dispersions are detailed, and the factors that influence the stack size are also discussed. In Section 4, the focus is on the discussion of different modes of coagulation of colloidal particles and the determination of critical coagulation concentration. The factors that may change the critical coagulation concentration are also brought out. In Section 5, the phenomena for sol-gel transition are dealt with, together with a discussion on the phase diagram where the domains of sol, repulsive gel, attractive gel, and flocs can clearly be seen. In Section 6, a short review is made on a series of experiments that monitored the process of upward expansion of initially compacted bentonite in a vertical test tube and on the modeling effort. It is followed with a discussion on the mechanisms of bentonite swelling and a mechanistic model that can accurately predict the swelling pressures of the bentonite-based materials in dilute solutions over a wide range of dry densities. In Section 7, the general pattern of extrusion and erosion of bentonite into fractures with seeping, low ionic strength water is analyzed, and the modeling effort is also commented, to highlight the importance of understanding floc formation from either colloidal gel or sol in flow-through fractures. The summary of the report is given in Section 8.

2 The colloidal properties of bentonite

Bentonite usually forms from weathering of volcanic ash, most often in the presence of water. It is an aluminium phyllosilicate, essentially impure clay consisting mostly of montmorillonite and about tens of percent of accessory minerals such as quartz, calcite and gypsum.

In what follows, we summarize the reviews of Luckham and Rossi (1999) and Lagay (2006) on clay minerals to get familiar with different terms and concepts that are key to understand the colloidal stability of bentonite when it is dispersed in dilute solutions.

2.1 Clay minerals and their structure

The inorganic fraction of soils and natural sediments consist almost entirely of silica and various silicates. Clay minerals are hydrous silicates or alumino silicates and may be defined as those minerals, which dominantly make up the colloidal fraction of soils, sediments, rocks and waters. They are distinguished from other colloidal materials by the highly anisometric and often irregular particle shape, the broad particle size distribution, the different types of charges (permanent charges on the faces, pH-dependent charges at the edges), the heterogeneity of the layer charges, the pronounced cation exchange capacity (CEC), the disarticulation (in case of smectites), the flexibility of the layers, and the different modes of aggregation (van Olphen, 1977; Lagaly, 2006). As they occur in nature, clays consist of a heterogeneous mixture of finely divided minerals, such as quartz, feldspars, calcite, etc., but the most colloidally active components are one or more species of clay minerals.

The structural framework of the clay minerals is basically composed of layers comprising silica and alumina sheets joined together and stacked on top of each other. Two structural units are, as illustrated in Fig. 1, involved in the atomic lattices of most clay minerals. One unit is called the *octahedral sheet*. It consists of two sheets of closely packed oxygens and hydroxyls in which aluminum, iron or magnesium atoms are embedded in octahedral coordination, so that they are equidistant from six oxygens or hydroxyls. The second unit is built of silica tetrahedrons and is called the *tetrahedral sheet*. In each tetrahedron, a silicon atom is equidistant from four oxygen atoms, or hydroxyls if needed to balance the structure. The silica tetrahedral groups are arranged to form a hexagonal network, and is repeated indefinitely to form a sheet of composition $Si_4O_6(OH)_4$.

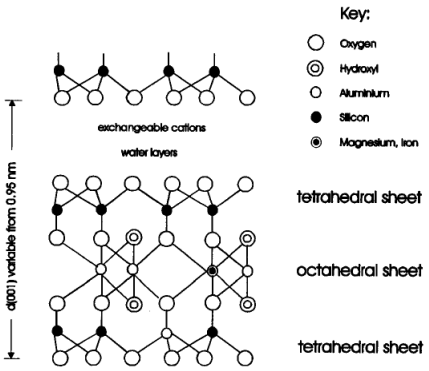

Figure 1. Schematic representation of the montmorillonite structure (Luckham and Rossi,

The analogous symmetry and dimensions in the tetrahedral and octahedral sheets allow the sharing of oxygen atoms between the sheets. In the case of the 'three-layer minerals' or *smectite* clay minerals, one alumina or magnesia sheet shares oxygen atoms with two silica sheets, one on each side. The combination of an octahedral sheet and one or two tetrahedral sheets is called a *unit layer*. Most clay minerals consist of unit layers that are stacked parallel to each other. A schematic representation of the atom arrangements in a unit cell for a three-layer clay, such as montmorillonite, is shown in Fig. 1. This structure is called the Hofmann structure. Within the unit layer the unit structure repeats itself in a lateral direction. This unit structure is also called a *unit cell*.

The unit layers are stacked together face-to-face to form what is known as the *crystal lattice*. The distance between the plane in one layer and the corresponding plane in the next layer is called the *basal spacing* or *c-spacing* d(001). The sheets in the unit layer are tied together by covalent bonds, so that the unit layer is stable. The layers in the crystal lattice are, however, held together only by Van der Waals forces and secondary valences between juxtaposed atoms. Therefore, the lattice cleaves along the basal surfaces, forming tiny mica flakes.

Noticeably, clay mineral crystals carry a charge arising from isomorphous substitutions of certain atoms in their structure for other atoms of a different valence. In the tetrahedral sheet, Si^{4+} may be replaced by trivalent cations (Al^{3+} or Fe^{3+}), or divalent cations (Mg^{2+} or Fe^{2+}) may replace Al^{3+} in the octahedral sheet. When this is the case, a charge deficiency results and a negative potential at the surface of the clay is created, which is compensated by the adsorption of cations on the surface. At the crystal edges, cations and anions can also be held because the interruption of the crystal along the *c*-axis results in broken valence bonds. In aqueous suspension, both sets of ions may exchange with ions in the bulk solution. They are known as *exchangeable ions*. By far the cations dominate the amount of exchangeable ions, and the total amount of cations adsorbed on the clay, expressed in miliequivalents per hundred grams of dry clay, is commonly called the *cation exchange capacity* (CEC). It is an important characteristic of the clay material and a typical value for montmorillonite is 1 mol of univalent charge per kilogram of clay. The CEC is high for sodium montmorillonite, compared to the other clay minerals.

2.2 Types of clay minerals and montmorillonite

The most important types of clay minerals are: illites, kaolinites, attapulgites, chlorites and smectites (van Olphen, 1977). The first two types consist of plate-like particles that do not have an expanding lattice; therefore water does not penetrate between the layers by osmotic forces (these clays can, however, be separated into small particles surrounded by water). In illites, this is due to the strong interlayer bonding from the high layer charge, and in the case of kaolinite is due to the strong hydrogen bonding. Attapulgite particles consist of bundles of 'laths', which separate into individual laths (long shaped needles) when mixed vigorously with water. Consequently, the rheological or flow properties of attapulgite suspensions are dependent on mechanical interference between the long laths, rather than on electrostatic interparticle forces. Chlorites differ from the above in that they possess a positive charge on one layer, balanced by an additional negative charge. Thus, normally there is no interlayer water.

The smectite 2:l structural units are three-layer clay minerals in which one tetrahedral sheet of one unit layer is adjacent to another tetrahedral sheet of another layer. They are classified as 2:l phyllosilicates. In this case, the oxygen atoms are opposite one another and bonding between the layers is weak. Also there is a high repulsive potential on the surface of the layers resulting from isomorphous substitution. These two last factors contribute to the increase of the c-spacing between the layers due to the penetration of water. Thus, smectites have an expanding lattice, where all the layer surfaces are available for hydration and cation exchange. Interlayer surface and cation hydration between smectite structural units is a unique property of smectite clays.

As the best-known member of the smectite group, montmorillonite is classified in structure as *dioctahedral*, having two thirds of the octahedral sites occupied by trivalent cations. Dioctahedral montmorillonite has its structural charge originating from the substitution of Mg^{2+} for $A1^{3+}$ in the octahedral sheet, as illustrated in Fig. 1. The average layer charge of montmorillonite with an idealised structural formula of $M_y^+ nH_2O(Al_{2y}Mg_y)Si_4O_{10}(OH)_2$ varies between 0.2 and 0.4 eq/formula unit $(Si,Al)_4O_{10}$, but most montmorillonites have layer charges around 0.3 eq/formula unit corresponding to a surface charge density of 0.10 C/m^2. This negative charge is balanced by cations intercalated between the structural units and these cations may be alkaline earth ions (Ca^{2+} and Mg^{2+}) or the alkali metal Na^+. When Na^+ cations are exclusively in exchange with the montmorillonite surface, the clay is known as Na^+-montmorillonite (the expanding lattice may provide the clay with a specific area of as high as 800 m^2/g).

Additionally, as mentioned above, charges may also arise from adsorption or dissociation of protons at the crystal edges depending on the pH of the dispersion as in the case of oxides. In practice, there is a strong possibility that in a neutral clay suspension a positive double layer is created on the edge surfaces owing to the exposed alumina sheet, whereby it may become more positive with decreasing pH (an excess of protons creates positive edge charges) and its sign may be reversed with increasing pH (negative charges are produced by the dissociation of silanol and aluminol groups). Various studies indicate that the edges of clay particles are positively charged at pH < 7-8 and some data suggest that the edges are neutralised at pH ~ 6. The existence of positive sites on the edges have been demonstrated by the addition of a negative gold sols to the clay-type kaolinite, where the resulting electron-micrograph showed the gold particles adsorbing only at the crystal edges (Luckham and Rossi, 1999).

3 Delamination of montmorillonite particles in dispersions

In the strict sense, however, smectite (and other clay minerals) particles are never crystals. A smectite ‘crystal’ is more equivalent to an assemblage of silicate layers (which we call sheets) than to a true crystal (Fig. 2). Montmorillonite particles seen in the electron microscope never have the regular shape of real crystals but look like paper torn into irregular pieces (Lagaly, 2006). The core of the particles is surrounded by disordered and bent sheets with frayed edges. Layers or thin particles of a few layers protrude from the packets and enclose wedge-shape pores. The particles reveal many points of weak contacts between the stacks of the layers. At these ‘breaking points’ the particles may easily disintegrate during interlayer reactions, or as a result of mechanical forces that influence rheological behavior.

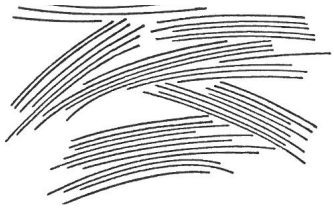

Figure 2. A schematic view of montmorillonite particles (Lagaly, 2006).

When dispersed in a dilute solution with alkali cations, preferentially Li^+ and Na^+, as the exchangeable cations to form a *colloidally stable suspension*, montmorillonite particles may be delaminated into individual sheets or thin packets of them (Fig. 3). In such a dispersion, it was found that the average interparticle distance (obtained from small-angle scattering) responded to the addition of sodium salts in an almost linear decrease with $2/\sqrt{c}$ (c = salt concentration) until, at $c \approx 0.2$ mol/l, particle rearrangement occurs and the basal spacing abruptly decreases from about 4 to 2 nm.

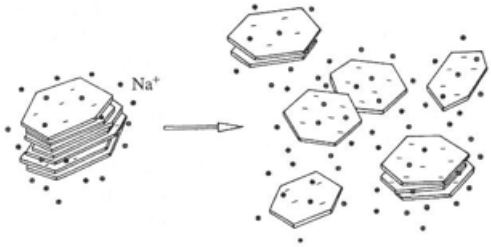

Figure 3. Disarticulation (delamination) of alkali montmorillonite particles in aqueous dispersions (Lagaly, 2006).

With cations other than Li^+ and Na^+ the distances separating individual layers are no longer equal but vary around a mean value. Particles are formed by a columnar-like superposition of a few sheets at equal distances and may be referred to as *stacks* of montmorillonite. The distances between these stacks are larger than within these units. Fig. 4 shows the relative number N/N_{Li} of layers per stack ($N_{Li} = 1$ for Li^+ as the exchangeable cation) when the Ca^{2+} ions are progressively replaced by alkali and Mg^{2+} ions (Schramm and Kwak, 1982). In the presence of Ca^{2+} ions the stacks contain about seven sheets. Even small amount (≤ 0.2 equivalent fractions) of alkali metal ions reduce the size of the stacks to one to three layers.

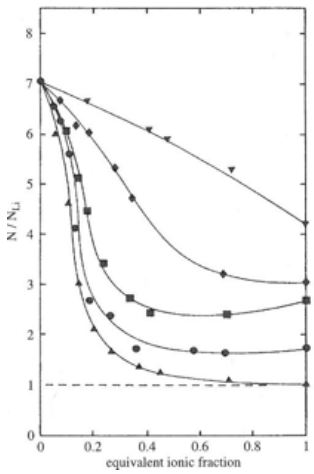

Figure 4. Relative number of layers per particle, N/N_{Li} (N_{Li} = 1) as a function of surface coverage when the Ca^{2+} ions are exchanged by Li^{+} (upward-pointing triangles), Na^{+} (circles), K^{+} (squares), Cs^{+} (diamonds), and Mg^{2+} (downward-pointing triangles) ions (Schramm and Kwak, 1982).

To understand the reason that results in the formation of montmorillonite stacks in water or dilute solutions, Liu (2015) recently developed a self-consistent approach of the weighted correlation approximation (WCA) to density functional theory and applied it to evaluate the interaction pressure between two infinitely large, plate-like colloidal particles. The results, based on the restricted primitive model (Wang et al., 2011) of electrolyte, are shown in Fig. 5 for a system involving both mono- and divalent counter-ions.

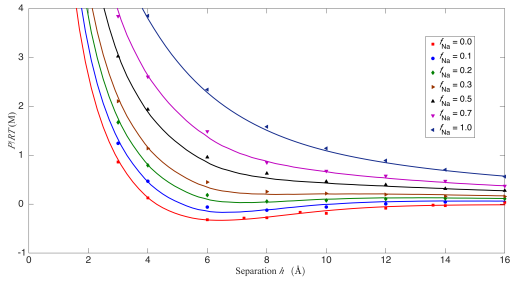

Figure 5. The pressure between two planar charged walls (with a surface charge density of -0.11 C/m^2) as a function of separation for a salt-free system involving both mono- and divalent counter-ions. The solid markers show the results from MC simulations and the curves are from the self-consistent WCA calculations. The fraction of surface charge compensated by monovalent counter-ions in the solution is indicated in the figure (Liu, 2015).

It was found that the Monte-Carlo (MC) and self-consistent WCA results agree excellently with each other in the cases relevant to montmorillonite dispersions. More importantly, Fig. 5 shows that the competition between the counter-ions makes the clay always swelling in a way much like purified and fully Na-exchanged bentonites when the fraction of surface charge compensated by monovalent counterions f_{Na} is greater than 30%. The larger the Na fractional surface coverage is, the stronger the monotonic repulsion between the clay particles becomes. In the opposite situation when Ca^{2+} dominates with f_{Na} < 30%, a shallow minimum is always

present on the pressure curve leading to an attraction that favors the formation of stacks in the clay system. The less the Na fractional surface coverage is, the more sheets the stack contains, making Ca-dominated bentonites very limited in swelling. In a clay system with only divalent counter-ions, a surface charge density around -0.08 C/m^2 (not accounting for the van der Waals interaction) is sufficient to aggregate the clay particles in a face-to-face orientation into stacks incorporating a water layer of ~ 1.0 nm.

Compared to the results shown in Fig. 4, one may conclude that the number of sheets per stack is closely correlated to the value of the shallow minimum of the pressure curves. This minimum serves as a sign of attraction resulting from ion-ion correlations. An enhanced attraction between the clay particles with less monovalent counter-ions leads to a large size of the stacks of montmorillonite. The stack sizes reduced from seven layers at f_{Na} = 0% to two layers at f_{Na} = 30%, and changed slightly with further increase in f_{Na} when the pressure has become a monotonically decreasing function of separation.

Hence, the formation of stacks in montmorillonite dispersions is a consequence of ion-ion correlations, which lead to a very weak repulsive or even attractive interaction between the outer sheets of the stacks. In the case involving a salt reservoir of finite concentration that dissociates into both counter-ions and co-ions, the study of Wang et al. (2011) from the application of the WCA on the basis of the bulk-fluid perturbation method also found similar results, as shown in Fig. 6.

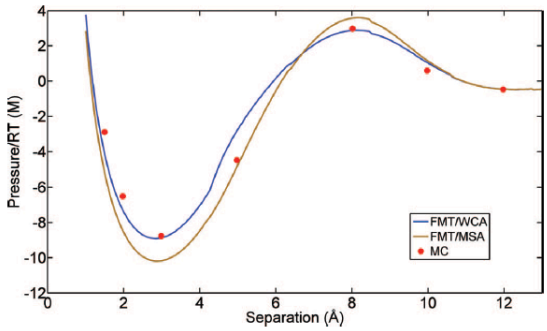

Figure 6. The pressure between two planar charged walls (with a surface charge density of -0.267 C/m^2) as a function of separation for the case involving a salt reservoir of 2.0 M 2:2 electrolyte. The solid markers show the results from MC simulations and the curves are from the FMT/WCA and FMT/MSA approaches, respectively (Wang et al., 2011).

The observation that stacks with many sheets are formed in dilute dispersions with Ca^{2+} as dominating cations can, therefore, be explained by the ion-ion correlation effects. However, if all layers or particles of montmorillonite were equally affected by such an effect, a total collapse of the sheets would be expected and a rigid body with about 50 % porosity would be generated. This is, nevertheless, not the case due perhaps to the fact that the sheets are heterogeneous in both size and charge distributions and that the surface charge is discretely distributed in each of the sheets. The MC studies of Khan et al. (2005) strongly indicated that, if discrete surface charges were considered, attractive forces between the sheets with smeared out surface charges would be weakened and can even be turned into a repulsive force. As a result, one may expect that when stacks are formed the outer layers of a stack does not attract another stack but repel each other (see Section 6).

In addition, it should be stressed that due to the inherent limitations of the restrictive primitive model, the results shown in Figs. 5 and 6 cannot be used to explain the dependence of the average number of sheets per stack on the size of montmorillonite particles. More recently, using small angle X-ray scattering and osmotic stress techniques, Segad et al. (2012, 2015) investigated the stack formation and the swelling behavior of montmorillonite particles from three different sources, Wyoming, Bavaria and Slovakia (the particle size distributions in natural bentonite vary significantly). They found that, in the presence of divalent counter-ions, the sheetss of montmorillonite aggregate into well-ordered stacks of limited size and with a well-defined spacing of 1 nm between the sheets. The stack size increases with the effective size of montmorillonite particles, as shown in Fig. 7. However, no stack formation was observed if the particles are too small, e.g. ~ 30 nm, irrespective of the montmorillonite origin and concentration of divalent ions.

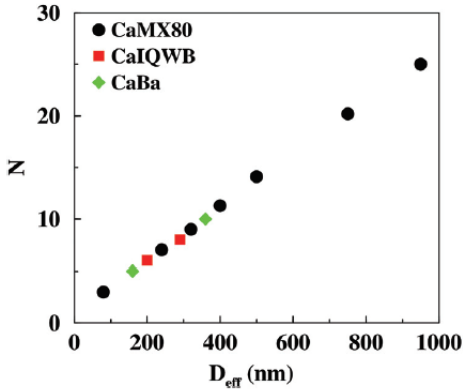

Figure 7. The average number of sheets per stack, *N*, as a function of the effective size of montmorillonite particles, D_{eff}, for size fractionated clays of different natural origin (Segad et al., 2015).

In addition, the formation and dissociation of stacks seem to be a reversible process. A large proportion of small particles in a mixed-size system affect the stack formation, reducing the aggregation number and increasing the inter-stack swelling in the system.

4 Coagulation of colloidal clay dispersions

Clay particles in suspension owe their stability to mutual repulsion when their intersecting diffuse double layers interact on approach (van Olphen, 1977; Lagaly, 2006). In clay-water systems, a double layer is made up of the negative surface charge and the balancing cation charge. In the case of clay particles, the negative charge is a consequence of imperfections within the interior of the crystal lattice. As discussed in Section 2.2, clay colloids possess a constant surface charge, because it arises from isomorphous substitution.

The counter-ions are electrostatically attracted by the oppositely charged surface. These ions have a tendency to diffuse away from the surface to the bulk solution where the concentration is lower. Therefore, the concentration of the counter-ions near the particle surface is high, and it decreases with increasing distance from the surface. The diffuse layer does not only consist of an excess of ions of opposite sign; there is a deficiency of ions of the same sign near the surface, since the ions are electrostatically repelled by the surface. This diffuse character of

the counter-ion atmosphere was recognised by Gouy and Chapman (van Olphen, 1977), who presented a theoretical treatment of the counter-ion distribution.

The surface charge of clay particles does not change with increasing electrolyte concentration; simply the diffuse double layer is compressed. The degree of compression of the double layer is governed by the concentration and valence of ions of opposite sign from that of the surface charge. The higher the concentration and the valence of the ions of opposite sign, the more the double layer is compressed. At high concentrations of sodium (Na^{+}) ions where the sheets approach to close distances (≤ 10 Å), the structure of the diffuse layer changes. Instead of two opposite diffuse layers of counter-ions between the approaching surfaces, one central layer forms and electrostatic attraction is created. Rearrangement of the counterions occurs at approximately 0.25 M NaCl and varies somewhat with the type of smectite (Luckham and Rossi, 1999).

The Gouy-Chapman theory leads, however, to unrealistically large ion concentrations at high potentials, since it assumes that the counter-ions are point charges. To correct for this, Stern (van Olphen, 1977) postulated the existence of an adsorbed layer of finite sized counter-ions adjacent to the surface. The potential in the Stern layer falls off linearly from its surface value to the Stern potential, after which it decays exponentially. The thickness of the Stern layer has been estimated for different clay systems. The outer Helmholtz plane lies outside the Stern layer and marks the boundary between the fixed and mobile part of the diffuse double layer, and is called the plane of shear. At this plane the potential is called the zeta potential and in practice it is assumed that it is equal to the Stern potential. This is a useful approximation of the considerably more complex conditions in the diffuse double layer.

The edge of the clay particle is, however, assumed to possess an electrical double layer of a different nature to that of the flat surface described above. As discussed in Section 2.2, this double layer results actually from the adsorption of potential determining ions on the broken bonds of the tetrahedral silica sheets and octahedral alumina sheets, and thus is pH-dependent.

Based on these understandings, a theoretical analysis of the interaction between colloidal particles has been developed by Derjaguin and Landau (1941) and Verwey and Overbeek (1948). The fundamental feature of what is known as the DLVO theory is that this interaction is determined by a combination of the inter-particle double layer repulsion energy and the van der Waals attractive energy (van Olphen, 1977). As discussed below, colloidal stability is commonly explained by means of the superposition of both energies.

4.1 Experimental observations

In a dilute clay suspension, the particles are suspended in pure water and do not agglomerate, due to the interaction of the diffuse double layers. In the presence of an electrolyte, however, the particles may approach each other so closely that they flocculate or coagulate. The critical concentration of electrolyte at which this occurs is usually known as the *critical coagulation concentration* (ccc) and is one of the most important characteristics of a colloidal dispersion.

Experimental results indicate that the higher the valence of the cations (either on the clay or in the salt), the lower the ccc value is. The very strong influence of the valence of the counter-

ions is typical of electrostatically stabilized dispersions. As seen in Table 1, well-dispersed clay minerals in the sodium form may coagulate by very low concentrations of inorganic salts. The ccc of sodium chloride varies between 3 and 20 mmol/l for Na^+-montmorillonite at pH ~ 6.5 It increases with solid content. The 0.025% Na^+-montmorillonite dispersions were coagulated by 5 mmol/l sodium chloride, 0.4 mmol/l calcium chloride, and 0.08 mmol/l aluminium chloride. The 0.5% dispersions of Na^+-montmorillonite were coagulated, however, by 20 mmol/l sodium chloride, 3 mmol/l calcium chloride, and 1.5 mmol/l aluminium chloride, respectively.

Table 1. The c.c.c. of Na^+, Ca^{2+}, and Al^{3+} chloride for Na^+-montmorillonite dispersions (0.025, 0.5, 1.0% w/w solid content) at pH ~ 6.5 from test-tube tests (Lagaly, 2006)

Exchangeable cation	ccc (mmol/l)		
	0.025%	0.5%	1.0%
Na^+	5	15	20
Ca^{2+}	0.4	2	3
Al^{3+}	0.08	1	1.5

The ccc also depends on pH and the type of anion. As a function of pH, the ccc of Na^+-montmorillonite showed a plateau between pH 4 and pH 6-7, and increased at higher pH. The dispersion coagulated spontaneously at pH<3.5 and was destabilized by the base necessary to raise the pH above 10.5.

Nitrate instead of chloride increased ccc from 5 to 16 mmol/l and sodium sulphate to 18 mmol/l (0.025% dispersion). The influence of certain phosphates can be extremely strong. As it can bee seen in Table 2, Na_2HPO_4 and NaH_2PO_4 coagulated the 0.025% dispersion at 1100 and 460 mmol/l, respectively. Sodium diphosphate ($Na_4P_2O_7$) up to its solubility limit (~ 130 mmol/l) did not coagulate the dispersion. In contrast, sodium phosphate (Na_3PO_4) showed a very low coagulation concentration of 25 mmol/l because the dispersion was highly alkaline (pH 11.5-12) at the point of coagulation. NaOH also coagulated at 20 mmol/l. In contrast to the influence of chlorides and nitrates, the ccc of Na_2HPO_4 and NaH_2PO_4 decreased with increasing solid content.

Table 2. The c.c.c. of sodium salts for 0.025 and 2.0% Na^+-montmorillonite dispersions (w/w solid content) at pH ~ 6.5 from test-tube tests (Lagaly, 2006)

	ccc (mmol/l)		pH
	0.025%	2%	
NaCl	5	30	6.5
$NaNO_3$	16	12	6.5
Na_2SO_4	18	35	6.5
$NaHSO_4$	4	4	~ 5
Na_2HPO_4	1100	80	9
NaH_2PO_4	460	40	~ 5
Na_3PO_4	25	35	11.5
$Na_4P_2O_7$	-	-	10
NaOH	20	30	11.5, 12

4.2 Different modes of coagulation

The influence of electrolyte concentration and pH on the association of montmorillonite particles has been a topic of considerable interest. At a sufficiently high clay concentration and low electrolyte content, the platelets may flex according to their relative positions and the relative magnitude of their surface and edge potentials (Luckham and Rossi, 1999). When the edges are positive, the platelets flex towards a negative face. When the edges are negative, the platelets are forced to assume a more parallel type orientation (Lagaly, 2006). For this reason, the pH of the medium is an important parameter related to the gel structure of the suspension, giving rise to different modes of coagulation: face-to-face, edge-to-face and edge-to-edge (Fig. 8).

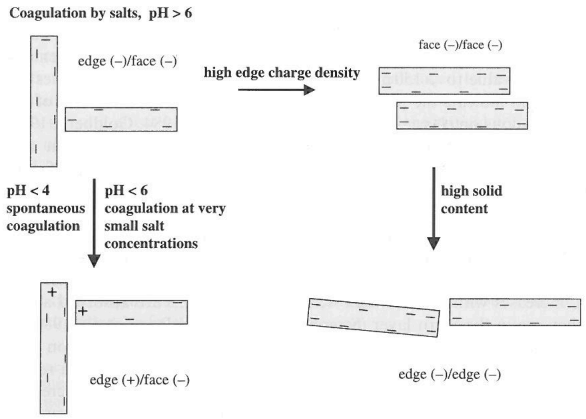

Figure 8. The different modes of coagulation of clay mineral particles (Lagaly, 2006).

The electrical interaction energy for these types of association is governed by three different combinations of the two double layers (Luckham and Rossi, 1999). Also, the rate of diffusion of the plate-like particles as they approach each other in these three ways is not the same, and they may not occur simultaneously or to the same extent when the suspension is flocculated. One can expect, however, that face-to-face association leads to thicker and larger stacks, and edge-to-face and edge-to-edge association lead to three-dimensional voluminous 'card-house' structures (Fig. 9). As illustrated in Fig. 8, the card-house mode of aggregation only forms when the edges are positively charged, or in a slightly alkaline medium above the ccc.

At pH ≈ 6.5, which is near or more likely above the point of zero charge of the edges, positive edge charges are no longer present or their number is very small. This, together with the fact that the negative double layer extending from the basal plane surface spills over into the edge region (the edge thickness of montmorillonite particles is small relative to the Debye-Hückel length at the ccc), leads to the interaction of negative edge charges with negative basal surface charges producing T-type contacts and card-house type aggregation (Fig. 9). The electrostatic repulsion between an edge (-) and a face (-) was, then, found on the basis of the DLVO theory to be distinctly smaller than between faces, even if the values of the charge density at the edges and the faces are assumed to be identical. As a result, the edge(-)/face(-) coagulation requires relatively low sodium salt concentrations, and the ccc values of montmorillonites, beidellites and illites are very similar (Lagaly, 2006).

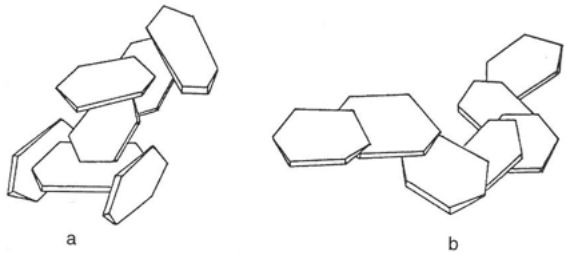

Figure 9. Aggregation of clay mineral layers in (a) card-house and (b) band-type networks by edge/face and face/face contacts (Lagaly, 2006).

With a weak increase of the edge charge density by adsorption of multivalent anions such as phosphate, the repulsive force between an edge (-) and a face (-) can be strongly increased, leading to a pronounced increase in the ccc value. When the increased salt concentration required for edge(-)/face(-) coagulation approximates the salt concentration for face(-)/face(-) aggregation, the dispersion coagulates face-to-face because the area between two faces is larger than between an edge and a face (face/face aggregation between two layers or particles might be initiated at surface regions with lower than average charge density because of layer charge heterogeneity).

Noticeably, transition from edge(-)/face(-) to face(-)/face(-) coagulation (Fig. 8), in particular at somewhat higher particle concentration, is promoted by the following effect. As discussed by Tateyama et al. (1988), edge(-)/face(-) attraction depends on the angle between the two particles and the particle thickness. This van der Waals attractive potential is very small for delaminated montmorillonite because the layers are only ~ 1 nm thick. Attraction becomes strong enough only for an almost perpendicular orientation of the two particles, which could be formed only at low particle concentrations. At higher concentrations, the strong repulsion

between the faces disrupts the edge(-)/face(-) contacts more easily and the attraction must be enhanced to reach the face(-)/face(-) coagulation condition. In the case involving dispersions with a high negative edge charge density of the particles, such a strong repulsion between the faces may even force the particles into adopting a certain parallel orientation, promoting edge (-)/edge(-) coagulation (Fig. 8). This is less likely to occur in dilute dispersions. Coagulation is then initiated when the interaction between the edges(-) becomes attractive, and it may include a certain overlapping of sheets forming band-type fragments (Fig. 9) in the pH range 6.9-13. As a result, coagulation requires much lower concentrations than those initiated by face(-)/face(-) interactions. This explains why the ccc of sodium hydrogen phosphates decreases markedly at higher montmorillonite contents (Table 2).

In comparison with sodium hydrogen phosphates and sodium diphosphate, sodium phosphate (Na_3PO_4) shows a very weak liquefying effect. The critical Na^+ concentration is $3\times25 = 75$ meq Na^+/l and therefore higher than for NaCl, $NaNO_3$, and NaOH, but distinctly lower than for Na_2HPO_4 and NaH_2PO_4 (Table 2). This is because the high pH (11.5) reduces the adsorption of phosphate by ligand exchange. The increase in negative edge charge density as a result of the high pH and modest adsorption of phosphate raises, then, the ccc values for edge(-)/face(-) coagulation but the increase is not sufficiently high to initiate face(-)/face(-) coagulation.

4.3 Theoretical estimation

As shown in Table 1, the ccc of Ca^{2+} and Al^{3+} counter-ions is distinctly smaller than that of Na^+ ions. The relationship between the ccc values is

$$ccc(Na^+) \approx 12\ ccc(Ca^{2+}) \approx 63\ ccc(Al^{3+})$$

while the extended DLVO theory predicts (Lagaly, 2006):

$$ccc(Me^+) \approx (4-64)\ ccc(Me^{2+}) \approx (9\text{-}729)\ ccc(Me^{3+})$$

where Me denotes a metal ion. The range of the predicted ccc values is related to different diffuse layer potentials. The smaller value corresponds to potentials ≤ 50 mV, and the larger value to ≥ 150 mV. Clearly, the observed ratios are near the values for lower potentials and indicate the pronounced effect of Stern-layer adsorption of the di- and trivalent cations on clay mineral surfaces.

The strong Stern-layer adsorption is also indicated by the increase in ccc values with solid content (Tables 1 and 2). When the salts solely regulate the thickness of the diffuse double layer, ccc would be independent of the solid content of the dispersion. However, ccc increases with solid content when the counter-ions are adsorbed at the surface, as they are in the Stern layer. On the other hand, the slightly increased ccc of $NaNO_3$ in comparison with NaCl may be explained by the water structure breaking effect of nitrate ions; as a result, the hydration of the cation increases and its adsorption in the Stern-layer decreases. Coagulation then requires a slightly higher salt concentration.

In this manner, the extended DLVO theory can well account for the effects of pH, the solid content, the type of anions, and the permanent charges etc. on the ccc of counter-ions. However, as pointed out by Liu et al. (2009a), the consequence of describing the electrical double layers as the Gouy-Stern type in the extended DLVO theory is that only a small but very relevant fraction of the counter-ions resides in the diffuse part of the double layers. The diffuse potential could actually be decreased to whatever degree, by allowing ion fluxes from one part of the electrical double layer to the other, in order to fulfill the requirement of sufficiently explaining experimental results. Furthermore, the implementation of spatial or surface charge regulations on the Gouy-Stern level might become increasingly complex and no longer facilitate the development of transparent analytical expressions. Instead, one must rely on numerical methods, not to mention the fact that additional efforts have to be made to determine some key parameters such as the intrinsic ionization constants, the density of adsorption sites, etc. The significance of the extended DLVO theory for practical use remains, therefore, somewhat academic as it does not lead to formulas that can be easily applied and are valid over a wide range of conditions.

For this reason, Liu et al. (2009a) attempted to estimate the ccc from a different point of view (without invoking the Gouy-Stern double layers) in the case of pH ~ 6.5. Considering in particular a test tube where colloidal expansion takes place, they understood that the ccc can be interpreted as the concentration of counter-ions below which expansion of colloids would always lead to full access to the entire volume of the test tube and above which a sharp boundary is established between a colloidal gel and pure water. Based on this perception and the dynamic force balance model (Liu et al., 2009b) that were developed earlier to describe colloidal expansion in a test tube, Liu et al. (2009a) derived an expression to approach the ccc by assuming homo-interaction at constant charge for montmorillonite dispersions. As shown in Fig. 10, the estimated ccc values agree quite well with those observed experimentally for both Na^+ and Ca^{2+} counter-ions at pH ~ 6.5, if accounting for the fact that montmorillonite particles mostly have a surface area close to 1.0×10^5 nm^2. This is in contrast to the classical DLVO theory, which over-predicts the ccc by about two orders of magnitude.

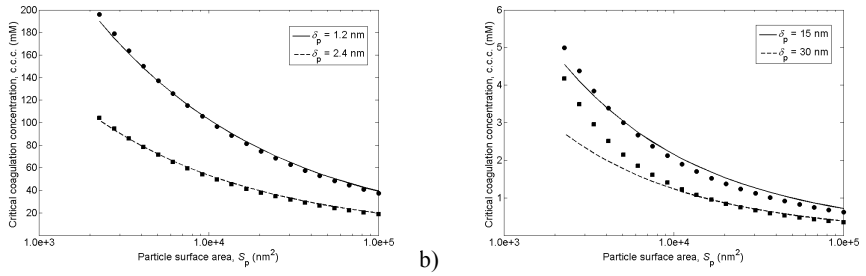

Figure 10. The ccc value as a function of the surface area of the particles for (a) monovalent and (b) divalent electrolytes, where the numerical results are represented by lines whereas the approximate results are shown by solid markers (Liu et al., 2009a).

Although this approach shares some features of the classical DLVO theory, it suggested that the ccc of counter-ions decreases with increasing surface area and with the thickness of the montmorillonite particles, and that the ccc is nearly independent of the surface charge density of the particles in the range of 0.069 ~ 0.137 C/m^2 (Lagaly, 2006). The influence of the solid content and the type of anions on the ccc, as discussed above, may then be attributed to the

stacking of sheets or band-type networks (Fig. 9), which increase both the surface area and the thickness of the montmorillonite particles on the average.

In practice, experimental studies strongly substantiated that addition of calcium ions into Na^+-montmorillonite dispersions has a pronounced effect on the type of aggregation. As discussed above, calcium ions held together the sheets at a maximum distance of 1 nm (basal spacing 2 nm). Even small amounts of calcium ions nucleate face/face contacts and build up band-type networks. The flow behavior of Ca^{2+}/Na^+-bentonite dispersions (discussed below) is therefore complex, and is sensitive to the ratio of Ca^{2+}/Na^+ in the dispersion.

Small amounts of calcium ions added to a Na^+-montmorillonite dispersion promote face/face contacts and stabilize band-type networks (Fig. 11b). At large amounts of calcium ions, the bands contract to form small aggregates, and eventually particle-like assemblages i.e. stacks, and the network falls apart (Fig. 11c). Homoionic Ca^{2+}-smectites thus show only a modest tendency for forming band-type networks.

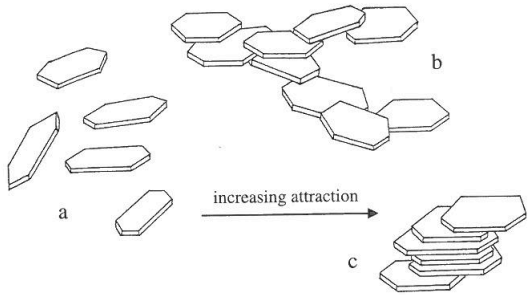

Figure 11. Aggregation of the clay mineral layers with increasing attraction: (a) single layers, (b) band-type aggregates, (c) stacks (Lagaly, 2006).

It may be assumed that calcium ions held between the negative charges at the edges and faces of two approaching particles act in a similar way as in the interlayer space and limit the particle distance to 2 nm (Lagaly, 2006). Stable edge(-)/Ca^{2+}/face(-) contacts would then be created that would build up a stable card-house network. However, this behavior seems very unlikely (calcium ions lying at the edges of particles with very irregular contour lines are in a quite different force field than between the planar sheets in the interlayer space).

5 Sol-gel transition

Transition from a sol into a gel and vice versa is very important in many practical applications because this phenomenon strongly influences flow behavior, sedimentation and filtration, and lies behind time-dependent rheological behavior.

Gels are usually described as dispersed systems that show a degree of stiffness. That is, the vessel containing the dispersion can be upturned without the dispersion flowing out. Gels also show a degree of elasticity, and creeping measurements may be used to distinguish between sol and gel (Lagaly, 2006). In general, it is expected that coagulation will cause the formation of a continuous gel structure instead of individual *flocs*, if the concentration of clay in a colloidally unstable suspension is high enough. The gel structures build up slowly with time,

as the particles orient themselves towards positions of minimum free energy under the influence of Brownian motion (Luckham and Rossi, 1999). The concentration of clay present in the system and the salt content are decisive factors in the length of time required for a gel to attain maximum strength.

As explained by the extended DLVO theory, gel formation at salt concentrations above the ccc is caused by attractive forces between the clay particles when the van der Waals attraction dominates the electrostatic repulsion (leading to 'attractive gel'). At lower salt concentration the interaction is attractive between edges(-) and edges(-) and between edges(-) and faces(-); at higher salt concentrations it becomes attractive between the faces(-). It is likely there is a continuous transitions from the edge(-)/face(-) (card-house) to the face(-)/face(-) aggregation (band-type structure). If the forces between the faces(-) are strongly attractive at high salt concentration, the network contracts and disintegrates (Fig. 11). Distinct particles or stacks form; the dispersion destabilizes forming flocs that settle into a sediment.

In the absence of salt or at very low salt concentrations, however, single sheets or stacks of them repel each other by electrostatic forces. When the particle concentration is sufficiently high (≥ 1% w/w for many Na^+-montmorillonite dispersions), the diffuse double layers around the sheets, or particles, restrict the translational and rotational motion of these units. As a result, the viscosity increases and the dispersion stiffens (Lagaly, 2006). That is, gels could also be formed at low salt concentrations and high montmorillonite contents due to the secondary electroviscous effect. This type of gel is called a 'repulsive gel' although this is incorrect because it is not the gel but the inter-particle force that is repulsive. Addition of salt reduces the thickness of the diffuse double layer, and hence increases the translational and rotational freedom of the particles; the particles become more mobile again and the gel turns into a sol.

The domains of sol, repulsive gel, attractive gel, and flocs are clearly seen in the phase diagrams shown in Fig. 12. The large domain of sol separates the two gel types. At this point, it should be emphasized that the ccc estimated by the extended DLVO theory (van Olphen, 1977; Lagaly, 2006) from a static point of view or by the approach of Liu et al. (2009a) from a dynamic point of view, as discussed in Section 4.3, corresponds actually to the critical salt concentration that causes attractive gel at particle concentrations far smaller than 2% (w/w).

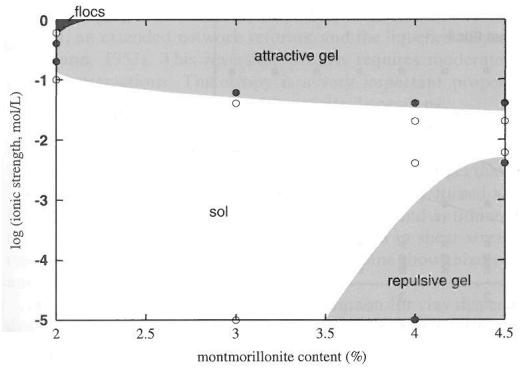

Figure 12. Sol-gel diagram for Na^+-montmorillonite (Wyoming type) and NaCl (Lagaly, 2006).

As seen in Fig. 12, the repulsive gel forms only when the particle concentration is > 3.5% (w/w) for Na^+-montmorillonite. The salt concentration at which the gel liquefies into the sol increases with particle concentration because more densely packed particles require thinner diffuse double layers to become mobile again. If there is attraction between the clay particles, the attractive gel might have smaller solid contents because band-type aggregates can span a distinctly larger volume.

Flocs are formed, however, only at the highest salt concentration and moderately high particle concentrations (the band-type aggregates are more stable resisting floc formation). For natural MX-80 bentonite, Neretnieks (2009) performed a series of scoping experiments on swelling of bentonite in downward sloping fractures. He observed that natural MX-80 bentonite as well as MX-80 washed of its gypsum content and homoionic calcium smectite could release clay flocs into initially deionised water, as demonstrated in Fig. 13. The water after some time in contact with the clay had acquired Na^+ and Ca^{2+} concentrations ranging form 0.42 to 2.9 and from 0.02 to 1.02 mM respectively.

Figure 13. Enlargement of the upside down turned slit 24 hours later after one of the experiments performed by Neretneiks (2009). Gel is slowly pulled downward by gravity. Small clay flocs are released and very slowly move downward. The whole picture is about 4 cm high.

In another series of experiments performed by Jansson (2009), floc formation was also clearly observed (Fig. 14) and used as a sign to estimate the ccc. As summarized by Neretnieks et al. (2009), some simple tests were made by Jansson (2009) where a small amount of clay (0.2 g) was put into the bottom of test tubes. 10 ml deionised water was poured onto the clay, which was allowed to swell and expand in water giving a volume fraction of smectite of 0.7 %. A thin very fine filter with nominal hole-size of 10 μm was fastened in the tube at the top of the gel/sol. The tubes were then filled to the rim with water with different compositions. After one day the tube was turned upside-down. The response was easy to observe visually within 5 minutes. Either the clay dispersed and started to fall through the net or else it stayed above the net. Some tubes where the clay stayed above the net were left for 1 month (for instance untreated MX-80 in deionised water) without anything happening.

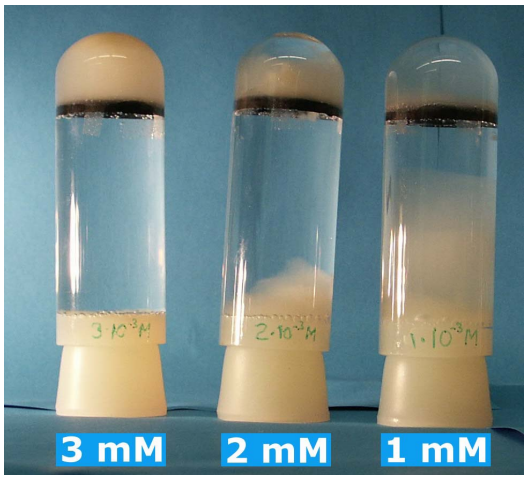

Figure 14. Observation of floc formation and determination of the lowest calcium concentration needed to keep homoionic Na^+-montmorillonite (Wyoming type) from dispersing (Jansson, 2009).

According to the tests performed, a calcium concentration of about 1 mmol/l is needed to stop the homoionic Na^+-montmorillonite particles from penetrating the filter. This is in agreement with common observations of the ccc of Ca^{2+} as dominating cations in water, as discussed in Section 4.1. It should, however, be pointed out that the notion of ccc is not well defined. For purified and Na exchanged bentonite contacted with calcium containing water, ion exchange will play a key role, as Na^+ intercalated between the sheets of montmorillonite will exchange for Ca^{2+} in the solution and then calcium would be ccc-determining ions, at least partly. More importantly, it was found from these tests that even at ionic strengths below the well-accepted ccc values the montmorillonite particles can agglomerate to form flocs that sediment much more rapidly than individual sheets can do (Neretnieks et al., 2015a; Neretnieks et al., 2015b). At the same time, such flocs can easily break up to pass very fine filters and recombine after passage. Although the underlying mechanisms are not yet sufficiently understood, Neretnieks (2015) recently discussed the effect of gravity and explored the consequence of floc formation on increasing the rate of bentonite loss from a deposition hole.

6 Swelling of bentonites

The discussions above describe mainly different mechanisms that govern colloidal stability and steady-state behavior of bentonite dispersions at low solid content. To see how the gel-sol transition develops in a closed system under the influence of bentonite swelling, a series of accurate observations have been made to monitor the process of upward expansion of initially compacted bentonite in a test tube (Dvinskikh et al., 2009), by use of the magnetic resonance imaging (MRI) technique. The general finding, as shown in Fig. 15, is that in distilled water the purified and fully Ca-exchanged bentonite, WyCa, swells more rapidly in the beginning than the other two bentonites but it stops expansion after only 1 day when it has expanded to about four times its original volume. By comparison, the purified and fully Na-exchanged bentonite, WyNa, always expands until the entire volume of the test tube has been occupied by colloidal particles. Within the full time period of measurements, however, the final state has not yet been reached, although WyNa has swollen to about 30 times its original volume. The swelling ability of MX-80 is somewhat in between WyNa and WyCa, but expands more

like WyNa in the sense that it continues to swell, albeit slowly, until at least some particles have reached the top of the test tube.

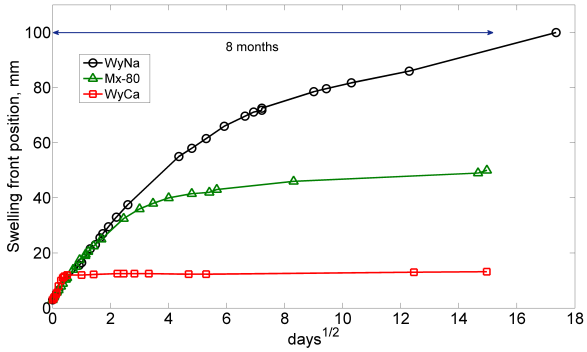

Figure 15. The propagation of the swelling front (the gel/sol interface) for different bentonites in de-ionized water (Dvinskikh et al., 2009). Note the horizontal scale of square root of time.

Using a dynamic force balance model developed for colloidal expansion (Liu et al., 2009b), it was found that the general features of the gel-sol transitions and the different behaviors of upward expansion of WyNa and MX-80 in distilled water or dilute solutions could be well followed in detail over a month (Liu, 2010; Liu et al., 2011), as illustrated in Fig. 16 for one case. When applied to simulate the upward expansion of WyCa in distilled water, however, significant deviations were observed between the predicted and measured results; the model cannot explain why WaCy stops expansion after only 1 day.

Since the model for colloidal expansion (Liu et al., 2009b) is developed on the basis of force balance between the van der Waals force, the electrostatic force, the thermal force giving rise to Brownian motion, the friction force, and gravity, one may attribute its failure in predicting WyCa upward expansion to the Poisson-Boltzmann description of the diffuse double layers. The reason for this is that the Poisson-Boltzmann model, on which the classical DLVO theory is based, does not account for the ion-ion correlations, the different processes of bentonite swelling and the formation of montmorillonite stacks in clay-water systems.

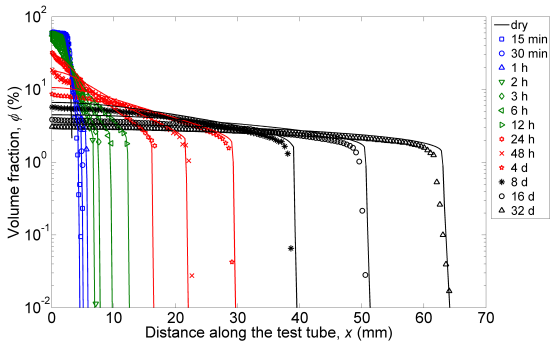

Figure 16. Measured versus predicted expansion of WyNa in a vertical test tube filled with 0.5mM $CaCl_2$ solution (Liu, 2010).

6.1 Mechanisms of bentonite swelling

As discussed in Section 3, in the structure of montmorillonite illustrated in Fig. 17, only a relatively small proportion of the inorganic cations balancing the negative layer charge are located at external crystal surfaces. The majority of these cations are present in the interlayer space between the clay platelets. The thin, negatively charged sheets are held together by the electrostatic forces between alternate layers of bridging cations (typically Na^+), forming stacks. When dry montmorillonite is placed in a moist atmosphere, it is able to take up water vapour by adsorbing it in the interlayer region. Swelling is the moving apart or disjoining of the clay particles, especially those in a parallel arrangement until they reach their equilibrium separation under a given pressure. The increase in the c-spacing, or the degree of expansion of the layer planes (Fig. 17), depends on the cations located in the interlayer region, i.e. on the basal cleavage. If the interlayer cations are monovalent and strongly hydrated (Na^+, Li^+), the inter-platelet repulsion is stronger and the degree of platelet separation is larger.

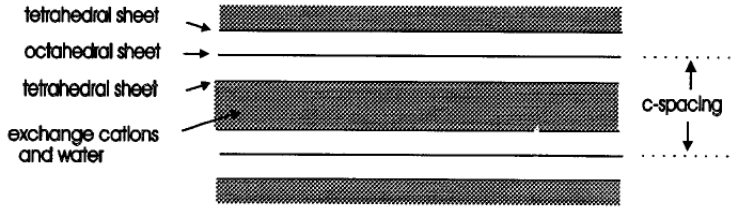

Figure 17. Schematic representation of a three-layer expanding clay lattice (Luckham and Rossi, 1999).

Depending on the extent of the increase in the basal spacing between two montmorillonite sheets, two types of swelling mechanisms may be distinguished: crystalline and osmotic swelling (Laird, 2006). *Crystalline swelling* results from the adsorption of monomolecular layers of water on the basal crystal surfaces (on both the external and interlayer surfaces). The first layer of water is held on the surface by hydrogen bonding to the hexagonal network of oxygen atoms. Montmorillonite is capable of intercalating a number of water layers and the c-spacing increases from 10 to 20 Å. Swelling in this region is primarily due to hydration of the interlayer cations that probably take up positions between two opposing sheetss. van Oss and Giese (1995) actually demonstrated, by applying a surface thermodynamic theory, that the Na^+-montmorillonite surface is hydrophilic, which also explains the large uptake of water between the platelets for this clay mineral.

Montmorillonite saturated with polyvalent cations such as Ca^{2+} do not normally expand beyond an interlayer separation of 10 Å, because the repulsive effect of ion hydration is offset by electrostatic attraction between the cation and silicate layers. However, montmorillonite containing small, monovalent cations, such as Na^+ or Li^+, can take up more water. The interlayer spacing may increase abruptly up to 30-40 Å and continues to increase to several hundred Angstroms with water content. This is called *osmotic swelling*. Its name comes from a repulsive osmotic force due to the interaction of the layers, limited only to some extent by van der Waals forces. A well-established phenomenon in Na^+-montmorillonite (in which the cations are particularly mobile) is, therefore, that the osmotic swelling can lead to complete exfoliation that would eventually break up the stack and form individual platelets (Salles et

al., 2008). In Ca dominated bentonite, however, the process of osmotic swelling is not as complete as that of Na^+-montmorillonite. The limiting dispersion state is, as discussed in Section 3, a collection of stacks in which the sheets remain separated by three or four layers of water molecules.

6.2 A mechanistic model of bentonite swelling

To explore if it is possible to take the most important mechanisms that govern the swelling of montmorillonite into account, while still using the Poisson-Boltzmann treatment of the diffuse double layers, Liu (2013) recently developed a mechanistic model. Aiming to suitably predict the swelling pressure of fully saturated, bentonite-based materials in distilled water or dilute saline solutions over a large range of final dry densities of bentonite, the model described the process of crystalline swelling with a thermodynamic relationship and the behavior of osmotic swelling with a diffuse double-layer model. It accounted, however, also for the disintegration of montmorillonite particles into small stacks upon water uptake. The idea behind the model is that although no theory could be used to predict the stack sizes as a function of bentonite properties, the interaction between the stacks that have been formed at the end of crystalline swelling can still well be described by the DLVO theory during osmotic swelling.

As exemplified in Figs. 18 and 19, comparison of the model predictions with a great number of experimental results of swelling pressures of different types of bentonites and bentonite-aggregate mixtures in both distilled water and dilute saline solutions suggests that the model works excellently in all the cases tested.

It was found that the water chemistry, the montmorillonite content, the type and amount of exchangeable cations in the interlayers are important in determining the extent to which the montmorillonite particles are delaminated and hence the swelling behavior of fully saturated, bentonite-based materials. However, the model did not take interstratification of several layer hydrates into account, but conceptualized the hydration of interlayer cations and the surface charge sites as a homogeneous process. This leads to the assumption of identical separation distances between the sheets within the montmorillonite particles, and as a result the size of the montmorillonite particles, i.e. the n_s value (the mean number of sheets per stack), may be underestimated somehow, particularly for Ca^{2+} dominated bentonites.

In practice, as illustrated in Fig. 19, the n_s value of stacked sheets of the montmorillonite particles in the region of 'fully developed' osmotic swelling was found to be in the range of 1 ~ 2.5 and 1.5 ~ 3.5 for Na^+ and Ca^{2+} dominated bentonites, respectively, saturated with distilled water. It appeared to increase with the amount of exchangeable cations of calcium and magnesium, but decrease when dilute saline solutions were used. In the case of Na^+ dominated bentonites saturated with 1 or 200 mmol/l NaCl, the particles of montmorillonite tend to break up easily, leading even to complete separation of the sheets. As a result, the previously developed diffuse double-layer models (e.g. Tripathy et al., 2004) are anticipated to give fair predictions of the swelling pressure, but this is definitely not the case when the average number of stacked sheets becomes greater than unity.

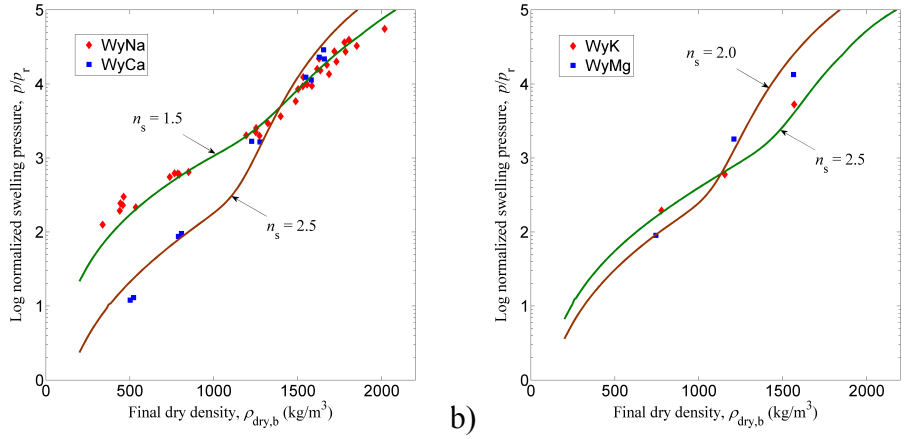

a) b)

Figure 18. Comparison of measured swelling pressure as a function of the final dry density of bentonite with the predicted pressure for a) WyNa and WyCa; and b) WyK and WyMg bentonites, respectively (Liu, 2013).

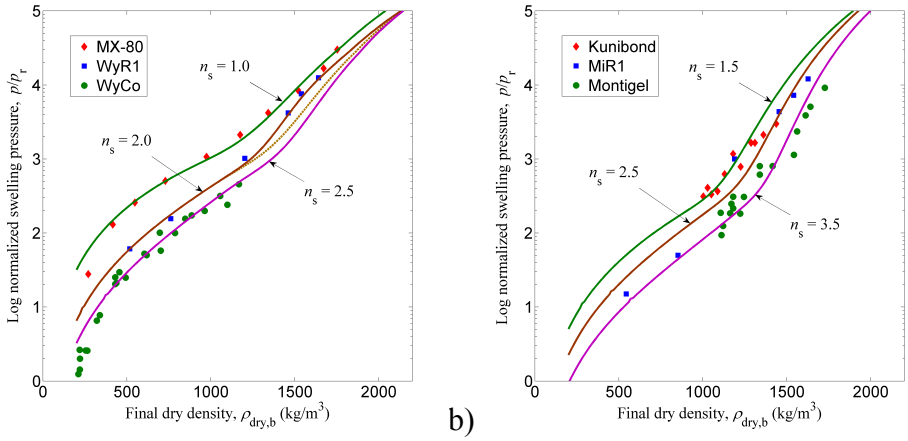

a) b)

Figure 19. Comparison of measured swelling pressure as a function of the final dry density of bentonite with the predicted pressure for a) sodium and b) calcium dominated bentonites, respectively (Liu, 2013).

It should, however, be stressed that despite its successes, the mechanistic model (Liu, 2013) may not be directly applied to the cases involving strong electrolytes. Nevertheless, with the use of this newly developed model, it is expected that the dynamic force balance model of Liu et al. (2009b) would give a better prediction of the upward expansion of initially compacted WyCa bentonite in dilute saline solutions in a test tube, at least qualitatively. This verification will be made in the near future.

7 Erosion of bentonites

The dynamic force balance model developed for colloidal expansion (Liu et al., 2009b) has also been applied to make a blind evaluation of the rate of erosion and loss of Na^+-bentonite from deposition holes for high-level nuclear waste (Moreno et al., 2011). The results show that the gel from compacted bentonite expanding into a fracture that intersect the deposition hole will flow with a non-negligible flow rate when its volume fraction is below 1%, but that

the erosion and loss of bentonite is not much influenced by the concentration of sodium in the clay or in the approaching seeping water, if they remain below the ccc value.

Partly to validate this model (Moreno et al., 2011) for bentonite erosion, and partly to observe how the gel/sol transformation develops in an open system with water flowing through a man-made fracture and if there is any significant change in the gel/sol transition pattern compared to the case of upward expansion, a number of experiments were recently performed (Schatz et al., 2012) under different conditions of water chemistry and flow rate. In these experiments, a compacted, cylindrical tablet of bentonite was allowed to expand into a flow-though, artificial fracture with a constant aperture of 1mm. The bentonite used was washed of detritus materials and was homoionic with either Na^{+} or Ca^{2+}.

As can be seen in the series of images presented in Fig. 20 for one test, the general pattern of bentonite erosion in low ionic strength water (below the ccc) is that a visible, erosive flow of solid material from around the extrudate develops; a distinct interface between the symmetric, inner zone of extruded material and the flowing, outer zone of eroding material can often be distinguished. The extruded material, appearing to have a cohesive, gel-like quality, extrudes rather uniformly out into the artificial fracture until a limiting distance of extrusion is reached. The eroding material, possessing a much more discrete, particle-like character, never becomes fully accessible to water flow. As a result, when the fracture was rotated at the end of test by 90° from a completely horizontal to a completely vertical position, the eroding material may rapidly sediment with gravity, indicative of particle sizes larger than those in the colloidal size range (< 2 μm). The extruded material shows, on the other hand, complete, static resistance to flow under gravitational load.

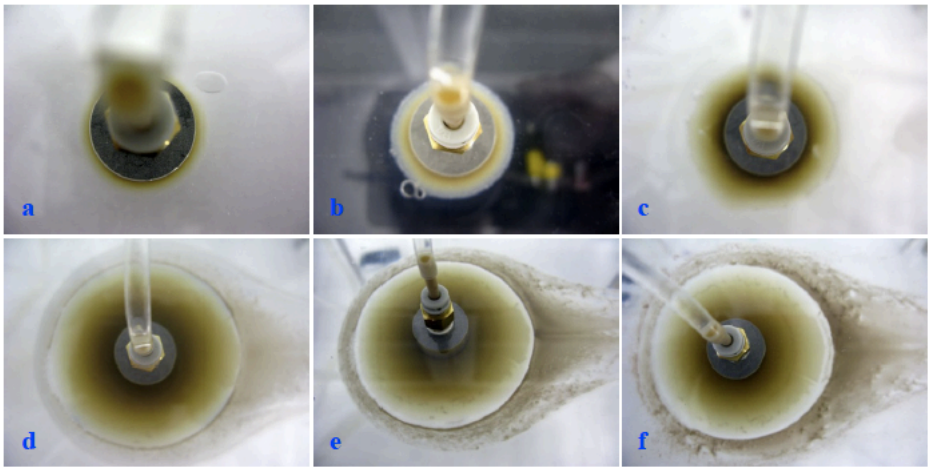

Figure 20. Overhead photographic images of a test involving sodium montmorillonite in deionized water at a) 1 h, b) 4 h, c) 24 h, d) 144 h, e) 312 h, and f) 456 h; the direction of flow in the 1 mm fracture is from left to right throughout the series (Schatz et al., 2012).

Of particular interest, it was found that in the cases with high flow rate the interface between the extruded and eroding zones is composed of discontinuous phases characterized by a built-up layer of particulate matter from which material is drawn into the eroding flow through the fracture, as shown in Fig. 21.

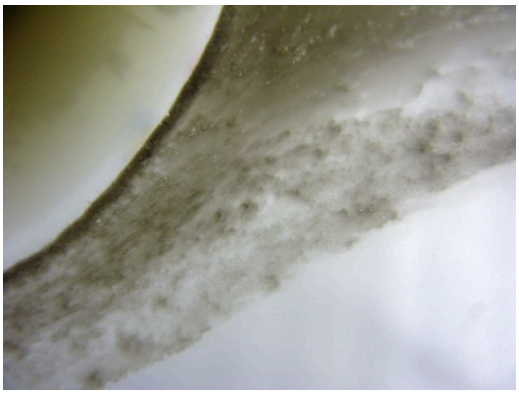

Figure 21. Close-up image of a test involving sodium montmorillonite in deionized water, which shows the interface between the inner zone of extruded material and the outer zone of eroding material (Schatz et al., 2012).

In other cases with low flow rate, however, there is no build-up of particulate matter directly at the interface. Instead, as seen in Fig. 22, a several mm wide, entirely transparent region was observed downstream of the gel-like extrudate and then particulate matter were formed and swept by the flowing water. This indicates that invisible, individual montmorillonite particles, which are released from the extruded material and are smaller than the wavelength of visible light, need time to form large enough agglomerates to become visible.

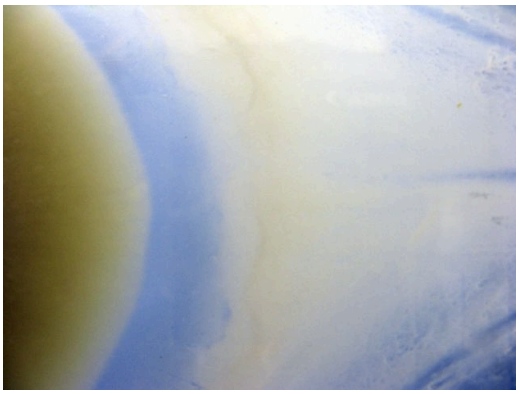

Figure 22. Close-up image of a test involving 50/50 calcium/sodium montmorillonite in deionized water, which shows the interface between the inner zone of extruded material and the outer zone of eroding material (Schatz et al., 2012).

One may, therefore, conceptualize the process of the extrusion and erosion of bentonite into fractures with seeping, low ionic strength water as one forms three, somewhat distinct zones with different properties, i.e. the gel/sol/floc zones. First, under the driving force of swelling, the hydrated bentonite expands/extrudes into the fracture, forming a zone where the extruded material is gradually transformed from a swelling paste into a gel. With a gradual decrease in density, the gel disperses and then turns into a colloidal sol, forming a zone where individual montmorillonite particles freely move (Fig. 22). Due perhaps to the effect of flowing water with velocity gradient, rapid collisions between individual particles lead to aggregation and a significant increase in density. The flocs or agglomerates thus generated are then drawn and swept into a zone of eroding flow. Depending on water chemistry and flow velocity, however, the sol zone may sometimes become so thin that it is entirely indistinguishable (Fig. 21), and

occasionally the layer of particulate matter at the interface may be rather diffuse; the flow of eroding material may then appear to have a fairly dispersed character (Schatz et al., 2012).

In the absence of water flow, as shown in Fig. 23, the floc zone does not appear at all. The expanding follows essentially the same pattern as that observed in the upward expansion test of Dvinskikh et al. (2009). This suggests that it is the water flow that enhances the collisions between individual montmorillonite particles in the sol zone, resulting in formation of flocs or agglomerates and subsequently the flow of eroding material in the flow-through experiments.

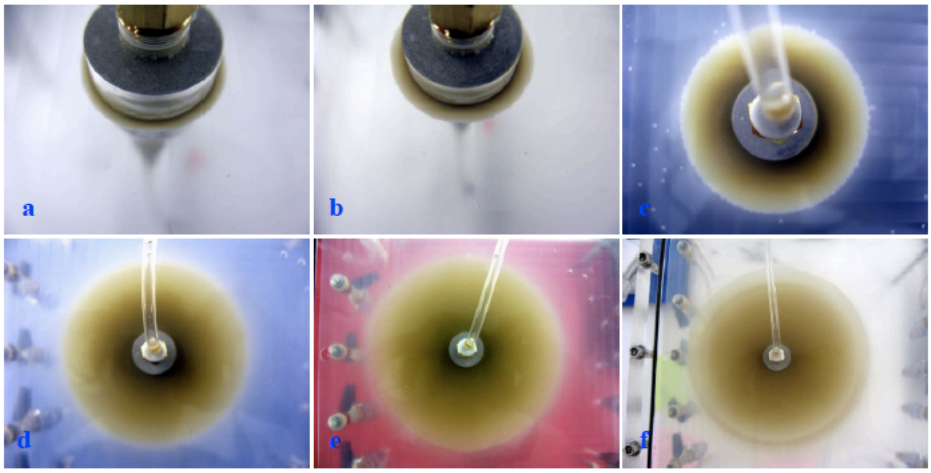

Figure 23. Overhead photographic images of a test involving sodium montmorillonite in deionized water at a) 15 min, b) 1 h, c) 24 h, d) 168 h, e) 384 h, and f) 720 h under stagnant conditions (Schatz et al., 2012).

Since the bentonite erosion model of Moreno et al. (2011) was developed on the basis of the dynamic force balance model for colloidal expansion (Liu et al., 2009b), it was not surprising to see that application of this model (Schatz et al., 2012) or a simplified version of this model - the two region model (Neretnieks et al., 2015a) gave fair predictions of the gel expansion and the erosive loss in the case shown in Fig. 23. However, in the flow-through cases (similar to the one shown in Fig. 20 with low ionic strength water) when agglomerates were clearly seen in the zone of eroding flow, the erosive loss was considerably underestimated and the rate of gel expansion was somewhat overestimated (Neretnieks et al., 2015a; Neretnieks et al., 2015b). This inconsistency is due perhaps to the fact that no mechanism for floc formation from the gel or the sol zone was accounted for in the models. More recently, Neretnieks et al. (2015a, 2015b) demonstrated that use of a simple means to invoke floc formation in the two-region model could make the predictions of both gel expansion and erosive loss very satisfactory. Hence, it would be of considerable value to better understand and quantify the process of floc formation from either gel or sol in a flow-through fracture system and also the behavior of flocs under gravity.

8 Summary

Based on our contributions (Liu, 2010; Liu, 2013; Liu, 2015; Liu et al., 2009a; Liu et al., 2009b; Liu et al., 2011; Moreno et al., 2011; Neretnieks, 2009; Neretnieks, 2015; Neretnieks et al., 2009; Neretnieks et al., 2015a; Neretnieks et al., 2015b; Wang et al., 2011) to the

research area of colloidal stability of clay dispersions and bentonite erosion, a review is made in the report on different mechanisms and factors that govern or influence colloidal stability of dispersions of natural bentonite in dilute solutions. Both experimental and theoretical studies on the process of the extrusion and erosion of bentonite into fractures with seeping water are also discussed in some detail. The aim is to bring out the importance of the delamination of montmorillonite particles, the card-house mode of aggregation, the sol-gel transition, and the floc formation in determining the stability of colloidal clay dispersions and also the erosive loss of bentonite into fractures that intersect deposition holes for high-level nuclear waste.

Acknowledgements

The work leading to this report has received funding from the European Atomic Energy Community's Seventh Framework Programme (FP7/2007-2011) under grant agreement n° 295487.

References

Derjaguin, B. and Landau, L., Theory of the stability of strongly charged lyphobic sols of the adhesion of strongly charged particles in solutions of electrolytes, *Acta Physiochem. URSS*, 14, 633 (1941).

Dvinskikh, S.V., Szutkowski, K., Furó, I., MRI profiles over very wide concentration ranges: application to swelling of a bentonite clay, *J. Magn. Res.*, 198, 146 (2009).

Jansson, M., Bentonite erosion-Laboratory studies, SKB Technical Report TR-09-33, Swedish Nuclear Fuel and Waste management Co., Stockholm, Sweden (2009).

Khan, M.O., Petris, S. and Chan, Y.C., The influence of discrete surface charges on the force between charged surfaces, *J. Chem. Phys.*, 122, 104705 (2005).

Lagaly, G., Colloid clay science, In: Bergaya, F., Theng, B.K.G., Lagaly, G. (eds), Handbook of Clay Science, Developments in Clay Science, Vol. 1, Elsevier, Amsterdam, Netherlands (2006).

Laird, D.A., Influence of layer charge on swelling of smectites, *Appl. Clay Sci.*, 34, 74 (2006).

Liu, L., Permeability and expansibility of sodium bentonite in dilute solutions, *Colloids Surf. A: Physicochem. Eng. Aspects*, 358, 68 (2010).

Liu, L., Prediction of swelling pressures of different types of bentonite in dilute solutions, *Colloids Surf. A: Physicochem. Eng. Aspects*, 317, 636 (2013).

Liu, L., Counterion-only electrical double layers: an application of density functional theory, *J. Chem. Phys.*, 143, 064902 (2015).

Liu, L., Moreno, L. and Neretnieks, I., A novel approach to determine the critical coagulation concentration of a colloidal dispersion with plate-like particles, *Langmuir*, 25, 688 (2009a).

Liu, L., Moreno, L. and Neretnieks, I., A dynamic force balance model for colloidal expansion and its DLVO-based application, *Langmuir*, 25, 679 (2009b).

Liu, L., Moreno, L. and Neretnieks, I., Permeability and expansibility of natural bentonite MX-80 in distilled water, *Phys. Chem. Earth*, 36, 1783 (2011).

Luckham, P.F. and Rossi, S., The colloidal and rheological properties of bentonite suspensions, *Adv. Colloid Interface Sci.*, 82, 43 (1999).

Moreno, L., Liu, L. and Neretnieks, I., Erosion of sodium bentonite by flow and colloid diffusion, *Phys. Chem. Earth*, 36, 1600 (2011).

Neretnieks I., Some scoping erosion experiments in thin slits between glass plates, Internal Report, Department of Chemical Engineering and Technology, Royal Institute of Technology, KTH, Stockholm, Sweden (2009).

Neretnieks I., Release and sedimentation of smectite agglomerates from bentonite gel/sol, Report to BELBaR Deliverable D5.3 (2015).

Neretnieks, I., Liu, L. and Moreno, L., Mechanisms and models for bentonite erosion, SKB Technical Report TR-09-35, Swedish Nuclear Fuel and Waste management Co., Stockholm, Sweden (2009).

Neretnieks, I., Moreno, L. and Liu, L., Evaluation of some erosion experiments by the two-region model, Report to BELBaR Deliverable D5.3 (2015a).

Neretnieks, I., Moreno, L. and Liu, L., Bentonite expansion and erosion – Development of a two-region model, Report to BELBaR Deliverable D5.3 (2015b).

Salles, F., Beurroies, I., Bildstein, O., Jullien, M., Raynal, J., Denoyel, R. and Van Damme, H., A calorimetric study of mesoscopic swelling and hydration sequence in solid Na montmorillonite, *Appl. Clay Sci.*, 39, 186 (2008).

Schatz, T., Kanerva, N., Martikainen, J., Sane, P., Olin, M., Seppälä, A. and Koskinen, K., Buffer erosion in dilute groundwater, Posiva Report 2012-44, Posiva Oy, Olkiluoto, Finland (2012).

Schramm, L.L. and Kwak, J.C.T., Influence of exchangeable cation composition on the size and shape of montmorillonite particles in dilute suspension, *Clays Clay Miner.*, 30, 40 (1982).

Segad, M., Cabane, B. and Jönsson, B., Reactivity, swelling and aggregation of mixed-size silicate nanoplatelets, *Nanoscale*, 7, 16290 (2015).

Segad, M., Jönsson, B. and Cabane, B., Tactoid formation in montmorillonite, J. Phys. Chem. C., 116, 25425 (2012).

SKB, Long-term safety for KB-3 repositories at Forsmark and Laxemar − a first evaluation, in: Main Report of the SR-Can Project, SKB Technical Report TR-06-09, Swedish Nuclear Fuel and Waste Management Co., Stockholm, Sweden (2006).

Tateyama, H., Hirosue, H., Nishimura, S., Tsunematsu, K., Jinnai, K. and Imagawa, K., Theoretical aspects of interaction between colloidal particles with various shapes in liquid, In: Mackenzie, J. D., Ulrich, D. R. (Eds.), Ultrastructure Processing of Advanced Ceramics, John Wiley & Sons, New York (1988).

Tripathy, S., Sridharan, A. and Schanz, T., Swelling pressures of compacted bentonites from diffuse double layer theory, *Can. Geotech. J.*, 41, 437 (2004).

van Olphen, H., An Introduction to Clay Colloid Chemistry: For Clay Technologists, Geologists, and Soil Scientists, John Wiley and Sons, New York (1977).

Van Oss, C.J. and Giese, R.F., The hydrophilicity and hydrophobicity of clay minerals, *Clays Clay Miner.*, 43, 474 (1995).

Verwey, E.J.W. and Overbeek, J.T.G., Theory of the Stability of Lyophobic Colloids: The Interaction of Sol Particles Having an Electric Double Layer, Elsevier, New York (1948).

Wang, Z., Liu, L. and Neretnieks, I., A novel method to describe the interaction pressure between charged plates with application of the weighted correlation approach, *J. Chem. Phys.*, 135, 244107 (2011).